CHAPTER 4

RESULTS AND DISCUSSION

4.1 Final design and model

Eventually, a RF MEMS piezoelectric vertical actuation micro relay was designed and modeled as shown in figure 4.0. Enlarged version of the figure and other details information are enclosed as appendices. Then its full geometry dimensions and modeler setting of its mechanical actuator path are summarized as in table 4.0. Though the signal path was not been simulated and analyzed due to the limitation of supporting software in the laboratory, but based on the paper “W-band finite CPW to microstrip line transition” which is presented by a group of researchers [19], the CPW-to-microstrip transition with straight coupling stubs is a W-band signal line where its return loss is better than -17dB from 85GHz to 100GHz. Furthermore, it was used in pair (back-to-back) in this design, but there is only part of microstrip was shown in figure 4.0 with a ground plane beneath to it and separated with a substrate. Based on the analyzer in appendix D, the microstrip line characteristic impedance is 51.537Ω and it is fulfilled the characteristic of a RF signal transmission line for lowest reflection from the load in order to have a perfect impedance matching [13].

For the actuator path, there are four terminals were used as electrodes, as shown in figure 4.0 which are two bottom electrodes and two top electrodes are common respectively. In other word, these bottom electrodes are to connect to the same terminal of a DC power supply and vice versa for the top electrode. Then the DC signal activates the inverse piezoelectric effect for the relay to switch vertically.

Then, this model was analyzed with a numerical method, and then its 3D CAD model was simulated by using SamCef Field_Oofelie ver. 5.2. Finally, the results generated were presented in the following sub-sections.

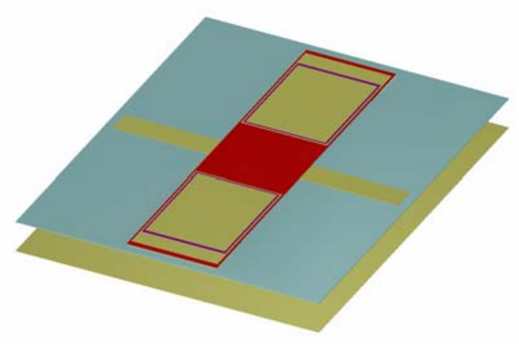

Figure 4.0: 3D model of a RF MEMS microrelay

Table 4.0: Piezoelectric actuator dimensions and modeler setting

Element	Volume	Bounding Box Size			Bounding Box Center	Max Tolerance
	μm^3	DX	DY	DZ	μm	μm
Contact Bar	2.43E+04	270	90.0002	1.0002	(0, 0, 101.5)	1.00E-04
Contact Passive Layer	1.22E+04	270	90.0002	0.5002	(0, 0, 102.25)	1.00E-04
Bottom Electrode 1	5.07E+04	260	390	0.5002	(0, -330, 104.25)	1.00E-04
Bottom Electrode 2	5.07E+04	260	390	0.5002	(0, 330, 104.25)	1.00E-04
Piezo Layer 1	4.13E+04	250	330	0.5002	(0, -305, 104.75)	1.00E-04
Piezo Layer 2	4.13E+04	250	330	0.5002	(0, 305, 104.75)	1.00E-04
Top Electrode 1	3.78E+04	240	315	0.5002	(0. -302.51, 105.25)	1.00E-04
Top Electrode 2	3.78E+04	240	315	0.5002	(0. 302.51, 105.25)	1.00E-04
Beam (Original)	3.85E+05	270	1080	2.0002	(0, 10, 103)	1.00E-04

4.2 Additional experiment and numeric analytical method

Based on the graph plotted from the experiment results, both of the displacements versus force showing a linear plotting, where it is represent able with $y = mx + c$ as in figure 4.1. According Hooke's Law, the force applied is equal to the force constant times its displacement as given in equation (3.7), where it force constant is $K = F/\delta(x)$. Then, ramp of the graph given in figure 4.1 is $m = \delta(x)/F$, where $m_{cantilver} = 0.3686$ and $m_{Bridge} = 0.1714$. Thus, its can be transformed into force constant by a inverse method. So that, the force constants are:

$$= \frac{1}{m_{Cantilever}} : \frac{1}{m_{Bridge}}$$
$$= 2.7130 : 5.8843$$
$$= 1 : 2.15$$
$$\approx 1 : 2$$

Hereby, it was proven that the bridge structural formed with combination of two cantilevers is equivalent to parallel stiffness connection as stated in equation (3.6).

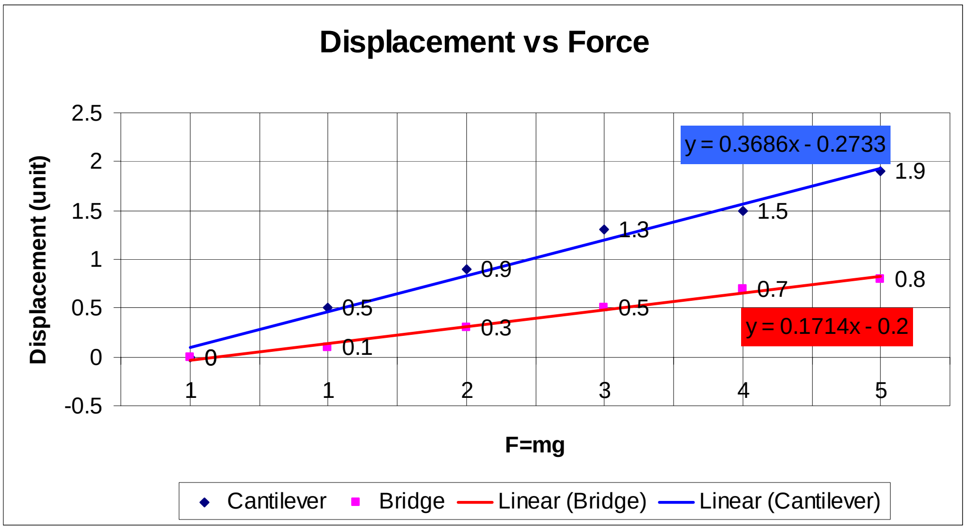

Figure 4.1: Experiment result

The behavior of the microrelay and the influence of the array configurations on the pull-in voltage and the contact force were analyzed. Greater force is needed to apply for a fixed displacement distance in bridge structural. According to figure 4.1, three unit of force was needed to make a 0.5unit displacement distance for bridge structural instead of 1 unit force for fixed-guided cantilever. Meaning that, greater energy such as higher driving voltage will be needed for bridge structural for a same displacement distance compare to cantilever beam. So another assumption made previously in sub-section 3.2.3.2 is applicable in its voltage estimation. According to figure 3.6, the contact force for the bridge structural to reach a stable contact was estimated as $F_B = F_1 + F_2$ where $F_{piezoactuator} = F_1 = F_2$. The numerical analyses data from section 3.2 was summarized in table 4.1.

Table 4.1: Numerical analytical data

Parameters	**Fixed-guided beam**	**Fixed-Fixed bridge**
Driving voltage for 2µm displacement (V)	~3.5	~7.0
Force constant, K (Nm^{-1})	1.0076	2.0152
Contact force, F (N)	2.0152E-6	4.0304E-6
Mass, M (kg)	4.2965E-10	8.5930E-10
Contactor resistance, R_B (Ω)	0.3	

4.3 CAD finite element method simulation

Four kinds of analyses under piezoelectric domain, linear static analysis, modal analysis, harmonic analysis and transient analysis have been completed by employing SAMCef Field Oofelie finite element software. However, no result is capable to be generated for the linear static analysis due to the multilayer structural because of it is analyzing how the device reacts statically to a constant voltage applied at the external faces of both piezoelectric layer and then it will demonstrate mainly how the beam deforms.

The main factor of the problem is caused by the absent assembly types in the CAD software which are used to assign the type of assemblies to the model before simulation. Unfortunately, there are only few of it are presenting in the software as shown in the appendix H. So, The multilayer mechanical path could not be assigned with the fixed assembly type, therefore multi devices were detected freely while simulation with the CAD software, and then its blocking each others from moving although the clamps constraint only applied at beam end face.

So, the analyses were only done for the single layer of the mechanical path which is the polysilicon beam for the rest analyses as discuses in the following sub-section without any voltage applied to it. The modal analysis had succeeded to determine the natural frequency for the polysilicon beam with a fixed-fixed condition. The actuation voltage and switching speed which are to be determined in harmonic response analysis and transient analysis respectively could not be performed, because of the same problem stated previously. Since the simulation was done without the bimorph layer and voltage supplied, then a prescribed displacement was set for further study of the beam vibration mode.

4.3.1 Modal Analysis

The first analysis was a modal analysis that is used to determine the vibration characteristic, such as the natural frequency and mode shapes of the beam. It was also a starting point for the harmonic analyses. The natural frequency and mode shapes are important parameters in designing of a structure for dynamic loading conditions. The best way of determining the vibration extracting modes is determining the specified frequency at which device will display range amplitude of vibration. So, the different coupled eigen modes and at which frequency they occur was identify. For this microrelay design, the first mode of the vibration showing the best suit vibration characteristic, and it was shown in figure 4.2. The vibration mode at 335.8695 kHz, the beam was deformed vertically, and the contact site which is located at the middle of the beam reached the maximum displacement which was shown with red color contour. For the rest mode shapes vibrating above the first mode resonant frequency had given the poor vibration characteristic and it were shown in appendix I.

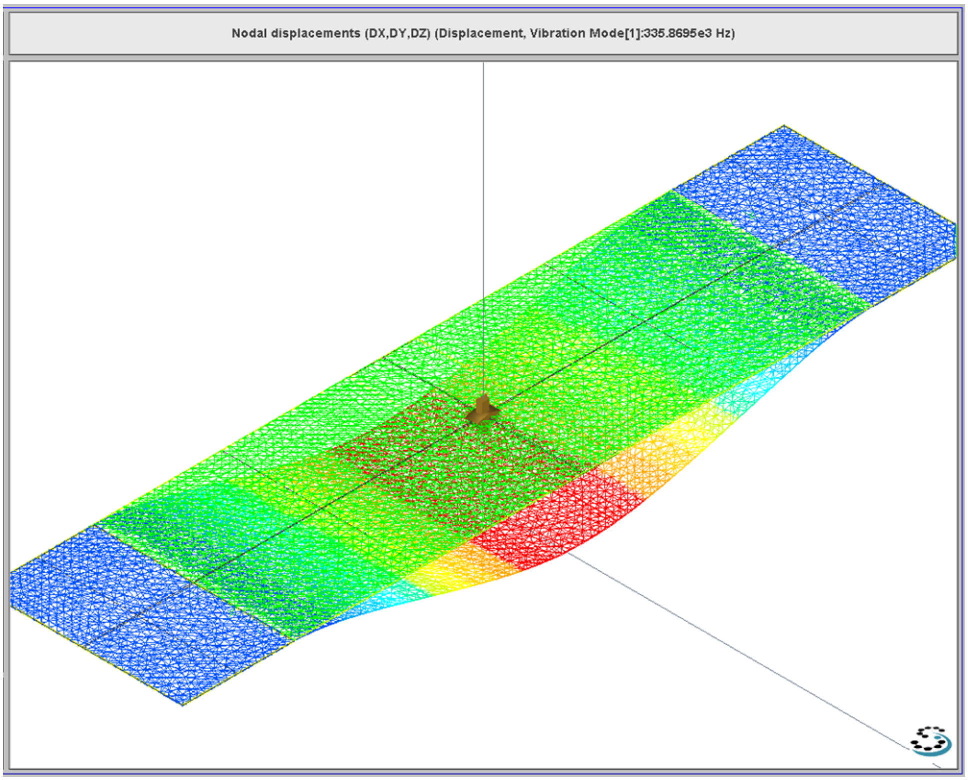

Figure 4.2: Modal analysis vibration mode at 335.8695 kHz

4.3.2 Harmonic response analysis with prescribed Displacement

In this stage, the actual behavior of the device over frequency range was analyzed. Since the beam will be remaining in static if no voltage was supplied to activate the inverse piezoelectric effect of the bimorph layer to generate piezo force, so a prescribed displacement was set to 2µm at the contactor bar. Then five nodes were selected along the beam to observe the vibration over frequencies from 0 to 5 MHz.

The vibration characteristics of the nodes were shown in figure 4.3. Node 808 which is indicated by green line was remaining constant at 2µm as prescription, but the other four nodes displacement varying over the frequency until greater than the available switching gap. Some of its displacement reached the maximum high about

200μm as shown in the figure below. As long as the vibration frequency below the resonant frequency which was determined at previous section about 335.9 kHz, the structural will be functioning properly, but once its exceed the limit, the mechanical structural will be self destroyed because the beam is impossible to reach the displacement at 200μm as given after 1.7 MHz. Its full displacement data over frequencies and few of the captures showing the vibration modes was enclosed in appendix J for further reference.

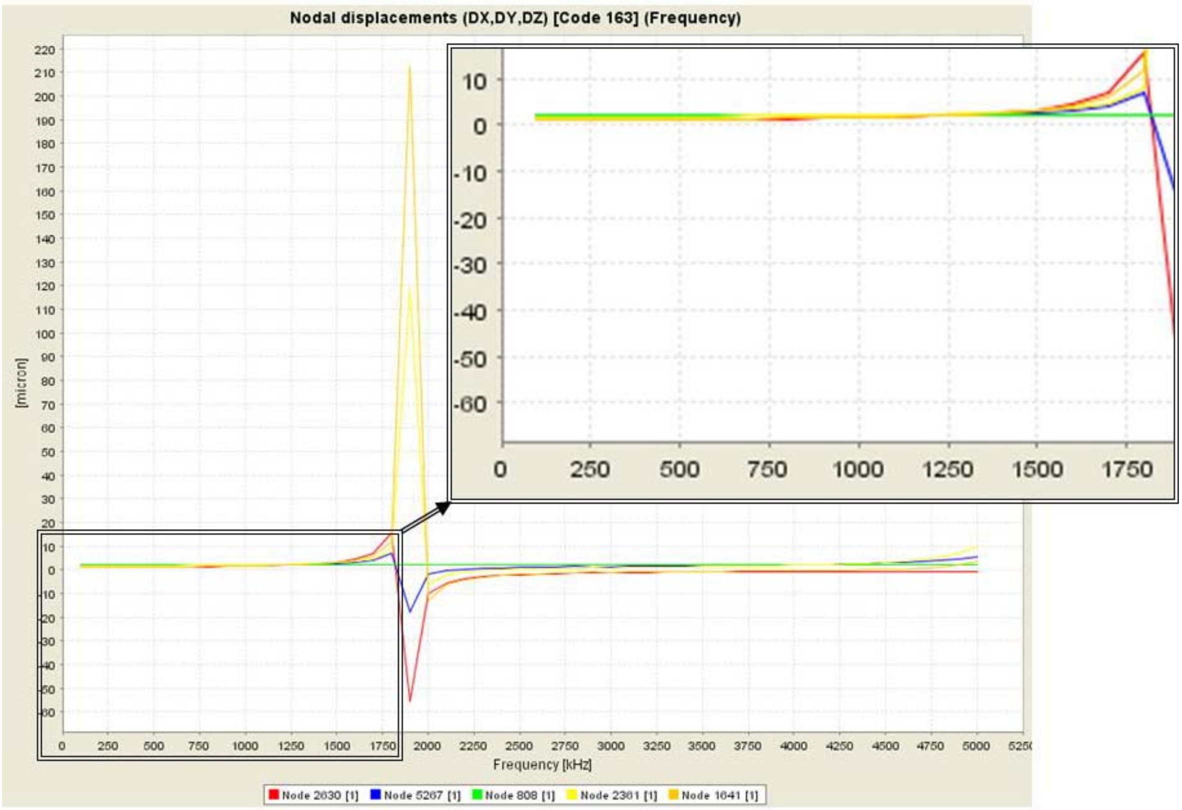

Figure 4.3: Nodal displacement vs frequency for a prescribed displacement

4.3.3 Transient Analysis with Prescription Displacement

As usual, no potential electric was included in this final analysis. So, the result is only showing the nodal displacement over time as in figure 4.4 with a 2μm prescribed displacement from 100μs-150μs. Then, six nodes were selected along the beam to observe the vibration over time to reach the steady state. Based on figure 4.4, the beam vibrated within the range from 0-0.2μm as indicated by the dark blue in the color contours of the color scale. The whole beam reached the steady state within 100μs for a single displacement.

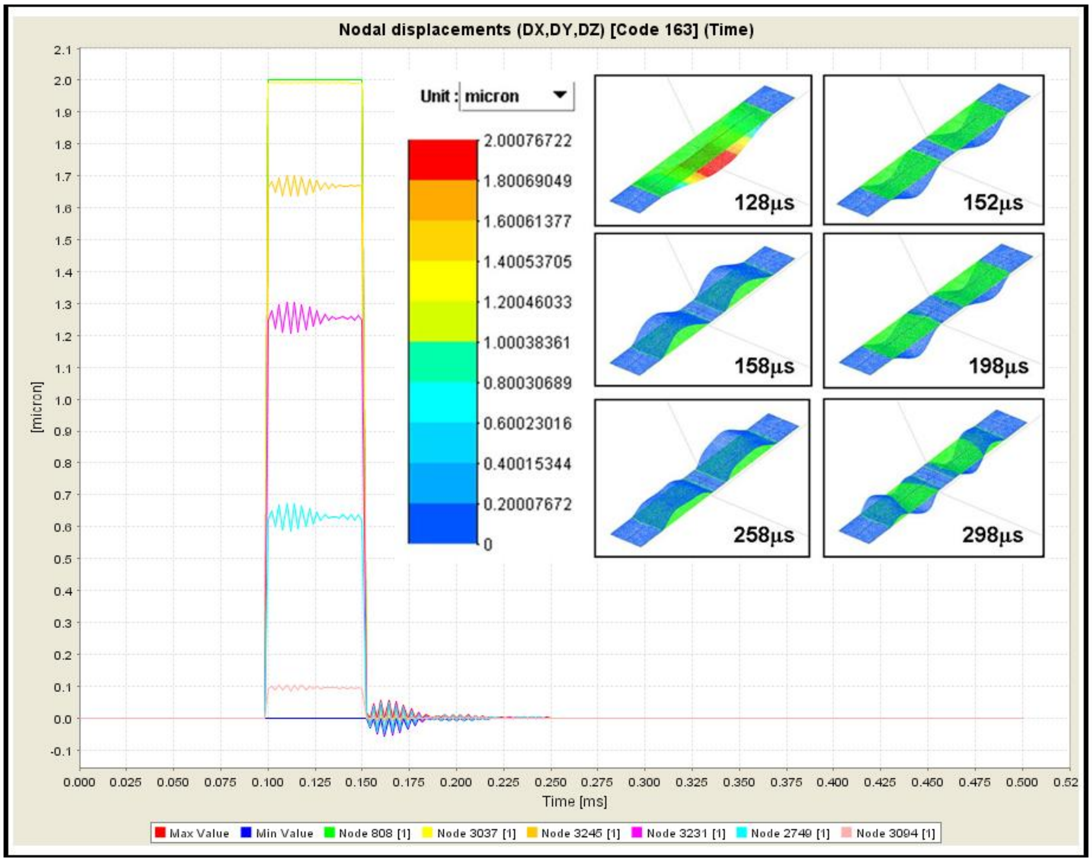

Figure 4.4: Nodal displacement vs time for a prescribed displacement

4.4 Possible optimizations

According to the modal analyses and harmonic response analyses done and the results showed that a sustained cyclic load will produce a sustained cyclic response, a harmonic response, in structural system. Harmonic response analysis can predict the sustained dynamic behavior of structures that will allows one to verify whether or not the design will successfully overcome resonance, fatigue, and other harmful effects or forced vibration.

However, the design still can be improved if it did not meet the specification. The resonant frequency of mechanical elements generally increases when scaled down as the value of M decreases rapidly based on the equation (3.9). Since the resonance frequency is a function of the device dimensions, it is susceptible to changes in temperature. Temperature stability can be achieved by temperature compensation [4]. This effect actually can be reached by creating holes in cantilever beam structure and this had been achieved and reported at [11]. Then, small settling time mean high switching speed, therefore, requires reducing the structure's mass/damping ratio. So, reducing the mass actually affected to increase both of the resonant frequency or natural frequency and its switching speed.

For this type of bimorph bridge structural used in designing the microrelay, if the mass of the structure is reduced by creating holes at the middle of the beam as shown in figure 4.5, the natural frequency of it was reduced to 300.3511 kHz compare to 335.8695 kHz of the original design. This is because of the holes created at the middle of the beam had changed the stiffness at the entire portion and worked as additional spring connected in series. Thus, it's reducing the force constant of the beam and hence greater displacement distance was achievable.

A trade off exists between voltage and resonance frequency for high device performance, such that low switching voltage also implies low switching speed. In other word, driving voltage and resonance frequency of the mechanical structure are variable due to its dimensions [11].

For those applications need greater contact force or bigger gap distance between contactor and the signal lines, the displacement capability of the actuator can be increased by using other piezoelectric material. An alternative material such as PZT discussed before during material selection at sub-section 3.2.2 was showed that it's capable to deform few times greater than ZnO at the same condition.

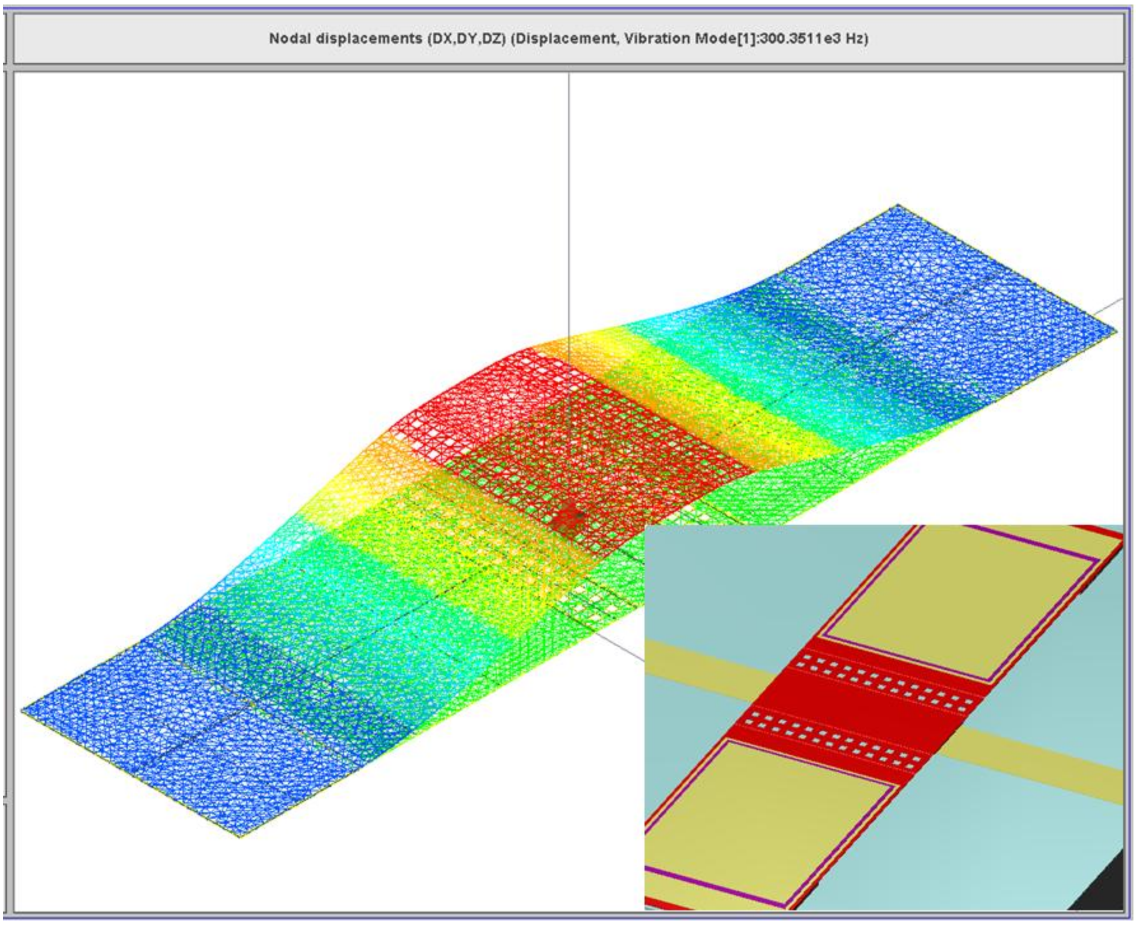

Figure 4.5: Effects of creating holes at the middle polysilicon beam

4.5 Limitations of the CAD software

After using SamCef Field Oofelie CAD software to simulate the device, it was found that some of the assembly types were not presenting in the software as stated before and shown in appendix H. Without the tool such as the fixed assembly type to be assigned as its data analysis, the software was not able to analyze the full multilayer sandwich structure as given by this microrelay mechanical path. Then, it caused incomplete and inaccurate simulation done on the device for a single layer of its polysilicon beam.

Beside that, this software also found not supporting complex geometry shape. The complex model was detected as invalid shape while simulation in progress, and then caused the analyses to be failed or stopped with no result displayed. This was more critical for the geometry with a lot fillet or chamfer edges.

For a CAD designed to use in MEMS such as SamCef Field Oofelie, it is found with another limitation in performing RF path analyses. Since it is only a FEM analyzer, then it is only capable in compute mechanical parameters. Other than that, the measurements will be done after the cleanroom fabrication processes with a real device, as being reported from most of the journalist or researchers in their papers.

4.6 Reliability design

Based on MUMPs processes, metal anchor should be placed in the design in order to ensure the metal layer stick rigidly with the other non metal layer during the fabrication process. Since the microrelay design is using the bimorph multi materials sandwich structure, and various materials have its own expansion rate and elastic capability. Then there is only piezo layer will be expanded with it stress generated form the piezoelectricity effect, and the elastic poly beam will be driven by the piezo stress and deform vertically. Due to extend it mechanical life time, metal anchors were needed to avoid the multilayer layers from loosing too fast over time. Other then that, a blanket of thin silicon nitride to cover the mechanical path is necessary. Then, this most outer layer will be used as the protective layer to the whole structure and also to create a more robust structure in anti fragile or loosing.